PHYSICAL REVIEW B **81**, 214432 (2010)

Magnetic coupling parameters at an oxide-oxide interface from first principles: Fe_2O_3-$FeTiO_3$

Hasan Sadat Nabi,[1,*] Richard J. Harrison,[2] and Rossitza Pentcheva[1]
[1]*Department of Earth and Environmental Sciences, Section Crystallography, University of Munich, Theresienstr. 41, 80333 Munich, Germany*
[2]*Department of Earth Sciences, University of Cambridge, Downing Street, Cambridge CB2 3EQ, United Kingdom*

(Received 26 December 2009; revised manuscript received 23 April 2010; published 21 June 2010)

Charge mismatch at the interface between canted antiferromagnetic hematite (α-Fe_2O_3) and antiferromagnetic ilmenite ($FeTiO_3$) is accommodated by the formation of mixed Fe^{2+} and Fe^{3+} contact layers, leading to uncompensated magnetic moments in the system. To derive the magnetic exchange interaction parameters of the end members and interface, we map total-energy differences of collinear spin arrangements obtained from density-functional theory calculations to a Heisenberg Hamiltonian using the least-squares method. Parameters for the end members, hematite ($J_m^{3+,3+}$) and ilmenite ($J_m^{2+,2+}$) are in good agreement with the values obtained from inelastic neutron-scattering data. The magnetic interaction parameters between Fe^{2+} and Fe^{3+} ($J_m^{2+,3+}$) in the contact layer show a strong antiferromagnetic coupling to the adjacent hematite layers and thus explain the ferrimagnetism in the system.

DOI: 10.1103/PhysRevB.81.214432 PACS number(s): 75.30.Et, 75.70.Cn, 75.47.Lx, 73.20.−r

I. INTRODUCTION

The polar discontinuity has been recognized as a driving force in the emergence of unexpected electronic phases at oxide interfaces. One example is the stable room-temperature remanent magnetization observed in nanoscale intergrowths of hematite and ilmenite.[1] In this system, the valence mismatch arises at the interface due to a stacking of $2Fe^{3+}/3O^{2-}$ in hematite and $2Fe^{2+}/3O^{2-}/2Ti^{4+}$ in ilmenite. Robinson *et al.*[2] proposed that magnetism emerges due to a mixture of Fe^{2+} and Fe^{3+} at the interface. Recent density-functional theory calculations with an on-site Coulomb repulsion term have provided theoretical evidence for this compensation mechanism and the resulting interface (lamellar) magnetism.[3] The study of Robinson *et al.*[2] was based on Monte Carlo (MC) simulations that used an empirical set of magnetic interaction parameters based on the untested assumption that Fe^{3+}-Fe^{2+} interactions (for which there are no literature data) should have the same sign but lower magnitudes than the corresponding Fe^{3+}-Fe^{3+} interactions (for which literature data exist).

Obtaining accurate magnetic exchange interaction parameters is thus essential in understanding and modeling the magnetic behavior of this material. Exchange interaction parameters can be derived, for example, by fitting inelastic neutron-scattering data to the theoretical dispersion-relation expression[4,5] and magnetic susceptibility.[6] On the other hand, first-principles calculations can be very useful to extract these quantities either by fitting total-energy differences of several magnetic configurations to a Heisenberg Hamiltonian[7–10] or by using the second variation in the total energy.[11] Such methods have been applied in the past to bulk materials or impurities in diluted magnetic semiconductors.[12] In this paper, we provide magnetic interaction parameters for an oxide interface, which are not accessible, e.g., from experiment.

Both end members, hematite (α-Fe_2O_3) and ilmenite ($FeTiO_3$), crystallize in a corundumlike structure with space group $R\bar{3}c$ and $R\bar{3}$, respectively. The oxygen ions form a distorted hexagonal-closed-packed lattice and cations occupy 2/3 of the octahedral sites resulting in buckled layers. Hematite is a canted antiferromagnet below 948 K: the Fe^{3+} spins lie in the basal plane (perpendicular to the *c*-axis) with antiferromagnetic (AFM) coupling between neighboring layers. A small spin canting above the Morin temperature ($T_M = 260$ K) results in a weak net magnetic moment within the basal plane. Below the Morin temperature, the orientation of spins switches to be almost parallel to the *c*-axis. Ilmenite is an antiferromagnet below $T_N = 55$ K: Fe^{2+} layers separated by magnetically inert Ti^{4+} layers couple antiferromagnetically with Fe^{2+} spins oriented parallel and antiparallel to the *c*-axis.

The magnetic interaction parameters extracted here from DFT calculations for the end members, Fe_2O_3 and $FeTiO_3$ are compared with available inelastic neutron-scattering data.[13–16] Previous theoretical work on Fe_2O_3 (Ref. 17) is also discussed. The main goal of the paper is to determine the magnetic interaction parameters between Fe^{2+} and Fe^{3+} at the hematite-ilmenite interface.

Briefly, in this paper Sec. II is devoted to details of the DFT calculation. Section III describes the method applied to extract the magnetic interaction parameters. The results for the bulk phases (Fe_2O_3 and $FeTiO_3$) as well as the interface are discussed together in Secs. III A and III B with implications for the magnetic properties of the interface. The main findings are summarized in Sec. IV.

II. CALCULATIONAL DETAILS

Density-functional theory calculations have been performed using the all-electron full-potential linear augmented plane-wave method as implemented in the WIEN2K code.[18] For the exchange-correlation potential, the GGA (Ref. 19) is used and electronic correlations are considered by including a Coulomb repulsion parameter *U* within the fully localized limit of LDA (local density approximation)/GGA (generalized gradient approximation)+*U* method.[20] For hematite, $U = 6$ eV and $J = 1$ eV is used to reproduce the experimental band gap while for ilmenite, $U=8$ eV and $J=1$ eV is needed. Thus the latter values have been used for $FeTiO_3$ and the intermediate members. In order to explore how the value of U affects the absolute values of the magnetic interaction, we have also performed calculations with $U=6$ eV. We note that similar values are typically used to describe iron bearing oxides.[21–24] For comparison, the U values obtained from constrained LDA (Ref. 25) for magnetite are 6.2 eV for Fe^{2+} in octahedral coordination and 7.69 and 8.73 eV for Fe^{3+} in a tetrahedral and octahedral site, respectively.[26]

The systems are modeled in a hexagonal unit cell with 30 atoms for Fe_2O_3 and 60 atoms for $FeTiO_3$ and intermediate members. The muffin-tin radii are 1.80 bohrs for Fe and Ti and 1.60 bohrs for oxygen. Inside the muffin tins, wave functions are expanded in spherical harmonics up to $l_{\text{max}}^{\text{wf}}=10$ and nonspherical contributions to the electron density and potential up to $l_{\text{max}}^{\text{pot.}}=6$ are used. The energy cutoff for the plane-wave representation in the interstitial is $E_{\text{max}}^{\text{wf}}=25$ Ry for the wave functions and $E_{\text{max}}^{\text{pot.}}=196$ Ry for the potential. For hematite and the intermediate members, the lattice parameters of hematite[27] ($a=5.04$ Å, $c=13.75$ Å) are used while for ilmenite, the corresponding bulk lattice constants of ilmenite[28] ($a=5.18$ Å, $c=14.27$ Å) are used. For each spin configuration, the internal degrees of freedom are fully relaxed.[29] For the integration in reciprocal space, we have used 24 and 15 k-points in the irreducible part of Brillouin zone for hematite and ilmenite, respectively. The convergence criteria ensure a numerical accuracy of energy differences better than 0.1 mRy/60-atom cell.

III. CALCULATION OF MAGNETIC INTERACTION PARAMETERS

In order to map the total energy from the DFT calculations onto a Heisenberg Hamiltonian, we separate it into a nonmagnetic (H_0) and magnetic contribution,

$$H=H_0-\frac{1}{2}\sum_{i,j}J_{ij}\mathbf{S}_i\cdot\mathbf{S}_j, \tag{1}$$

where the summation is over all distinct spin pairs. $\mathbf{S}_i$ is the spin vector at the ith lattice site and J_{ij} is the isotropic magnetic exchange interaction parameter between the magnetic moments on-site i and j. In the following, we use $J_{ij}=J_m^q(r_{ij})$, where the index m ranges from first to eighth neighbor and q defines the type of cations in the pair. For example, $J_m^{3+,3+}$ is an interaction between Fe^{3+}-Fe^{3+} pairs while $J_m^{2+,3+}$ is an interaction between Fe^{2+} and Fe^{3+}. $J_m^q<0(>0)$ corresponds to antiferromagnetic [ferromagnetic (FM)] coupling.

Figure 1 illustrates the magnetic pair exchange interactions which are used in our modeling. J_1 is the interlayer interaction between cations in face-sharing octahedra. J_2 is the intralayer interaction between cations in edge-sharing octahedra. J_3, J_4, and J_5 correspond to the interlayer interactions among cations with corner-sharing octahedra and J_6, J_7, and J_8 are the interactions with cations from the second-nearest layer.

Because we focus here on the properties of the Fe_2O_3-$FeTiO_3$ interface and not on the origin of spin canting of the end-member hematite which occurs above the Morin temperature, we have investigated only collinear magnetic configurations. Isotropic $J_m^q(r_{ij})$ are calculated by mapping the energy differences of these spin arrangements to the Heisenberg Hamiltonian in Eq. (1). The energy differences depend on the type of spin configuration: while some can be 10–40 mRy/30-atom cell, for hematite, the maximum energy difference between the ground-state AFM and a FM configuration is 250 mRy, consistent with the high magnetic ordering temperature of this material. The fitting of the DFT energy differences to the Hamiltonian is done by a multivariable least-squares (LS) method. The error bars for the obtained parameters from LS method are calculated within the confidence level of 0.99.

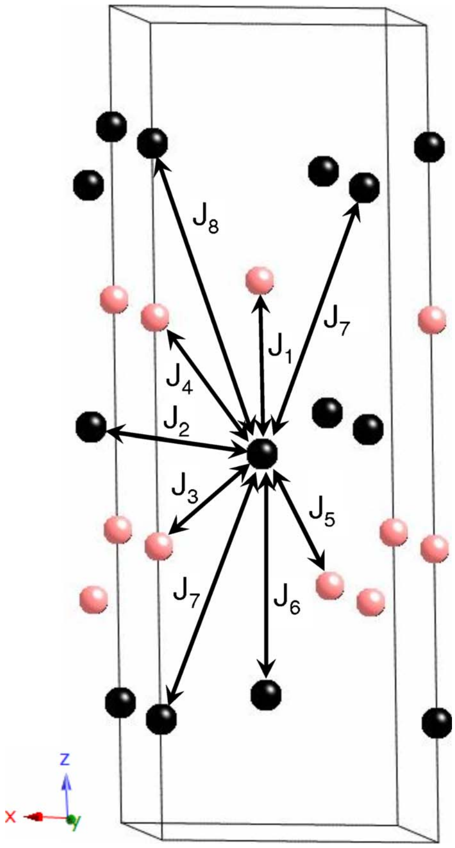

FIG. 1. (Color online) Side view of the corundum structure showing only the cation positions with alternating cationic layers denoted by light and dark atoms. Additionally, the pair magnetic exchange parameters J_1 to J_8 between the cations are defined.

A. Bulk phase: Fe_2O_3 and $FeTiO_3$

We first test the method for the end members for which we have calculated 23 and 10 different collinear spin arrangements, respectively. The calculated values for hematite ($J_m^{3+,3+}$) are displayed in Fig. 2(a) together with the values obtained from neutron scattering.[13] We find that for hematite, the dominant parameters are the interlayer magnetic interactions $J_3=-72$ K, $J_4=J_5=-50$ K. The negative sign implies a strong antiferromagnetic coupling between the Fe^{3+} layers and explains the AFM ground state of hematite. The values

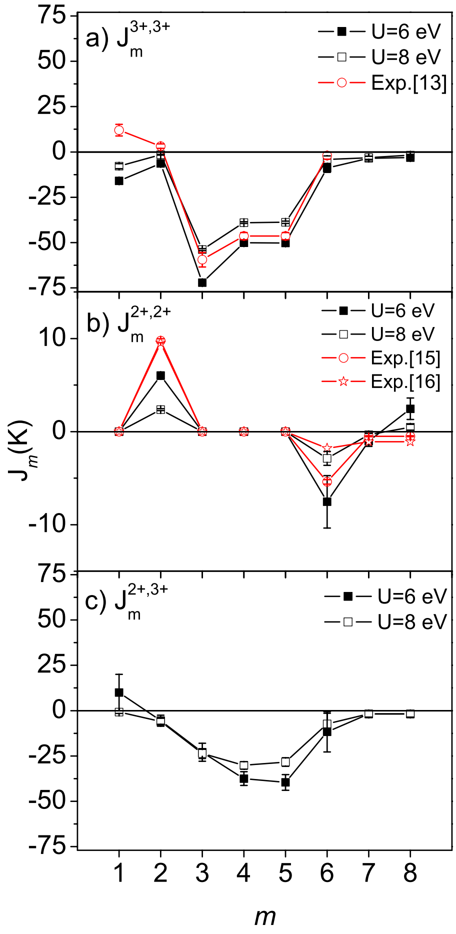

FIG. 2. (Color online) The magnetic pair interaction parameters $[J_m^q(K)]$ up to eighth neighbor are shown in (a) for hematite ($J_m^{3+,3+}$), (b) for ilmenite ($J_m^{2+,2+}$), and (c) for the interface ($J_m^{2+,3+}$). Results for $U=6$ and 8 eV are marked by filled and open squares, respectively. The experimental values for hematite (open red/gray circle) are taken from Ref. 13 and for ilmenite (open red/gray circles and stars) are taken from Refs. 15 and 16. The parameters for the interface in panel (c) are calculated for the configuration shown in Fig. 3(b).

TABLE I. Néel temperature for hematite and ilmenite calculated within the MFA and from Monte Carlo simulations for $U=6$ and 8 eV.

	Monte Carlo		MFA	
Material	$U=6$ eV	$U=8$ eV	$U=6$ eV	$U=8$ eV
Fe_2O_3	1150 ± 10	910 ± 10	1416 ± 41	1107 ± 37
$FeTiO_3$	50 ± 2	15 ± 5	43 ± 18	19 ± 5

are in good agreement both with the experimental data of Samuelsen and Shirane[13] as well as with previous LDA and LDA+U calculations by Mazurenko and Anisimov[17] who additionally took into account spin-orbit coupling. In contrast to experiment, J_1 and J_2 are found to be negative. However, both parameters are significantly smaller than J_3-J_5 and play therefore a minor role in the resulting magnetic ordering. Thus the strong interlayer AFM coupling enforces ferromagnetic coupling within each Fe^{3+} layer. Furthermore, our values support the reasoning of Goodenough[30] and Anderson[31] that cation interactions mediated by an anion (superexchange) with cation-anion-cation angles between $120°-180°$ (J_3,J_4,J_5) are negative in sign and much stronger than direct interactions between cations in face- (edge-) sharing octahedra, J_1 (J_2).

The calculated values for ilmenite ($J_m^{2+,2+}$) are shown in Fig. 2(b). In ilmenite, Fe^{2+} layers alternate with Ti^{4+} layers. Since Ti is in 4+ state (d^0), all the Fe-Ti interactions are zero (J_1, J_3, J_4, and J_5). The positive J_2 implies that magnetic interactions within the Fe^{2+} layer are ferromagnetic. On the other hand, J_6 and J_7 have a small negative value leading to an antiferromagnetic coupling with Fe in layers above and below the Ti layers. The positive J_2 and negative J_6 and J_7 determine the correct antiferromagnetic ground state for ilmenite. However, the absolute values are lower compared to the experimental ones obtained by Kato *et al.*[15,16] by fitting data at $T=12$ K to the magnon dispersion relation.

Useful comparisons with previous results for hematite can be made by calculating the Néel temperature using the mean-field approximation (MFA), defined as $k_B T^{MFA} = \frac{1}{3}S(S+1)\Sigma_m n_m J_m$, where k_B is the Boltzmann constant and n_m is the multiplicity of neighbors corresponding to J_m. It is an established fact that MFA cannot give the exact value for the transition temperature but provides a qualitative estimation. Using the MFA expression above and the spin magnetic moment of $S=5/2$ for Fe^{3+}, we obtain $T_N^{MFA}=1416 \pm 41$ K (1107 ± 37 K) for hematite with $U=6(8)$ eV, respectively (Table I). A previous DFT study[32] reported a higher value (1711 K). Both MFA values overestimate the experimental Néel temperature (953–966 K).[33] A recent LDA+DMFT (Dynamical Mean Field Theory) study obtained $T_N=1600$ K for hematite.[34] Monte Carlo simulations, following the method of Harrison[35] were used to obtain a more accurate estimate of $T_N=1150 \pm 10$ (910 ± 10) K for $U=6(8)$ eV, which are closer to the experimentally observed value. For ilmenite, the mean-field estimated temperatures using a spin magnetic moment of $S=4/2$ for Fe^{2+} with $U=6$ and 8 eV are $T_N^{MFA}=43 \pm 18$ and 19 ± 5 K. Monte Carlo (MC) simulations yielded a value of 50 ± 2 (15 ± 5) K for $U=6(8)$ eV.

The low Néel temperature for $U=8$ eV in ilmenite can be traced back to the small value of $J_2=2.4$ K, which is the interaction responsible for the ferromagnetic ordering within the Fe layers. Harrison *et al.*[36] found a value of $J_2=10.8$ K was required to obtain the correct Néel temperature for end-member ilmenite using Monte Carlo simulations, which is close to the empirical values obtained by Kato *et al.*[15,16] The low value of J_2 is likely due to the high on-site Coulomb parameter $U=8$ eV which was used in order to describe correctly the size of the band gap. Using $U=6$ eV, J_2 is significantly enhanced ($J_2=6.0$ K), resulting in a Néel temperature of 50 ± 2 K from MC simulations. A similar dependence of the magnetic interaction parameters on U is obtained for hematite and reported for Cr_2O_3.[9] For example, using $U=8$ eV instead of $U=6$ eV for hematite leads to a reduction in J_m ($m=3,4,5$) by ~20%.

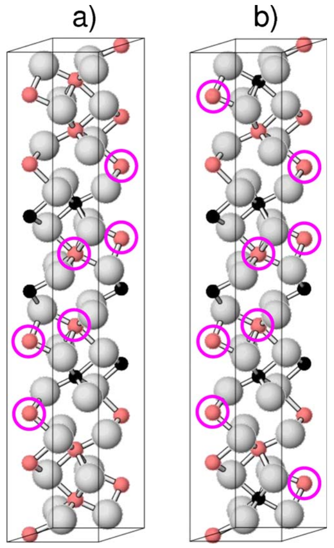

FIG. 3. (Color online) Side view of the configurations with 60 atoms in the unit cell chosen for the calculations of interface magnetic interaction parameters: (a) represents an ilmenite block (three Ti^{4+} layers separated by Fe^{2+} layers) within a hematite host and (b) contains additionally mixed Fe-Ti layers in the hematite part. The red, gray, and black spheres are showing Fe, Ti, and oxygen atoms, respectively. The positions of Fe^{2+} are marked with pink/gray circles and the rest of the iron are Fe^{3+}.

B. Magnetic interactions at the interface of Fe_2O_3 and $FeTiO_3$

As mentioned previously, a Fe^{3+} and Fe^{2+} contact layer is formed at the $Fe_2O_3/FeTiO_3$ interface as a result of the disruption of charge neutrality.[2,3] The sixth electron of Fe^{2+} occupies an a_{1g} orbital. This localized state is pinned at the Fermi level (for more details on the electronic properties, the reader is referred to Refs. 3 and 37). In order to extract the magnetic interaction parameters at the interface ($J_m^{2+,3+}$), we have considered several cation configurations. Figure 3(a) shows a heterostructure containing an ilmenite and a hematite block while Fig. 3(b) contains a layered part as well as mixed Fe-Ti layers. Because not all interaction parameters are accessible in the former (e.g., $J_{3,6}^{2+,3+}$), we have chosen the one in Fig. 3(b) to determine all $J_m^{2+,3+}$. For the latter, a total of 16 different spin arrangements were calculated.

The extracted parameters for the interface ($J_m^{2+,3+}$) together with the ones for the end members ($J_m^{3+,3+}$ and $J_m^{2+,2+}$) are displayed in Fig. 2 and Table II. Similar to hematite, we find that the dominant interaction parameters at the interface are J_3, J_4, and J_5. These have the same sign but are lower in magnitude than the corresponding Fe^{3+}-Fe^{3+} interactions. This result validates the main assumption made in previous Monte Carlo studies of the solid solution.[35,36] Although the absolute values of these interactions are generally smaller than in hematite, their negative value implies that Fe^{2+} in the contact layer couples antiferromagnetically to the next hematite layer. As a consequence, the direction of uncompensated magnetic moments at the interface will be pinned with respect to the hematite host, resulting in a ferrimagnetic behavior of the system. Monte Carlo simulations of magnetic ordering with a $4\times4\times4$ supercell were performed for the configuration in Fig. 3(a), which corresponds to the ground-state cation configuration for this bulk composition.[3] Magnetic transitions at 860 ± 10 (1080 ± 10) K were obtained in the hematite part of the heterostructure and 25 ± 5 (60 ± 5) K in ilmenite regions of the supercell with $U=8(6)$ eV, respectively, suggesting that the magnetic ordering temperature of both phases is modified by the presence of the interface.

The slight decrease in Néel temperature for hematite can be explained by the reduced strength of magnetic interactions in the contact layer ($J_m^{2+,3+}$) and a lower average number of interactions per cation due to the presence of the paramagnetic ilmenite. The increase in Néel temperature of ilmenite is likely caused by interaction of Fe^{2+} spins within the ilmenite lamellae with the magnetically ordered Fe^{2+}-Fe^{3+} spins within the contact layers.

IV. SUMMARY

The isotropic magnetic pair exchange interactions for the end members (hematite and ilmenite) are extracted from DFT calculations by mapping the total energies on a Heisen-

TABLE II. Isotropic magnetic pair exchange interactions in kelvin for hematite ($J_m^{3+,3+}$), ilmenite ($J_m^{2+,2+}$), and the interface ($J_m^{2+,3+}$) for $U=6$ and 8 eV. The index m describes the type of interaction following the definition in Fig. 1, n_m is the multiplicity of J_m. r_{ij}(Å) is the distance between the cations in each compound. Positive/negative signs of J_m^q correspond to FM/AFM coupling.

			$J_m^{3+,3+}$			$J_m^{2+,2+}$			$J_m^{2+,3+}$	
m	n_m	r_{ij} (Å)	$U=6$ eV	$U=8$ eV	r_{ij} (Å)	$U=6$ eV	$U=8$ eV	r_{ij} (Å)	$U=6$ eV	$U=8$ eV
1	1	2.86	-15.9 ± 1.6	-7.9 ± 1.4	2.92	0.0	0.0	2.84	10.0 ± 10.0	-0.8 ± 0.8
2	3	2.96	-6.3 ± 0.2	-1.5 ± 0.2	3.07	6.0 ± 0.4	2.4 ± 0.1	2.97	-5.5 ± 3.0	-5.9 ± 1.6
3	3	3.38	-72.1 ± 0.5	-53.8 ± 0.5	3.51	0.0	0.0	3.36	-23.0 ± 5.0	-23.7 ± 2.7
4	3	3.701	-50.1 ± 0.5	-39.0 ± 0.5	3.73	0.0	0.0	3.683	-37.5 ± 3.8	-30.2 ± 2.1
5	3	3.704	-50.2 ± 0.7	-38.8 ± 0.6	3.91	0.0	0.0	3.688	-39.6 ± 4.3	-28.4 ± 2.3
6	1	4.01	-9.0 ± 2.3	-4.3 ± 2.1	4.08	-7.5 ± 2.8	-2.9 ± 0.7	3.999	-11.7 ± 11.1	-7.4 ± 6.0
7	3	5.426	-3.4 ± 1.0	-3.2 ± 0.9	5.616	-1.0 ± 0.6	-0.3 ± 0.1	5.36	-1.9 ± 1.9	-1.8 ± 1.8
8	3	5.431	-3.1 ± 0.4	-1.7 ± 0.4	5.617	2.5 ± 1.2	0.5 ± 0.3	5.43	-1.9 ± 1.9	-1.8 ± 1.8

berg Hamiltonian. For hematite, we find a good agreement with experimental values from inelastic neutron-scattering data. For ilmenite, the ground state is reproduced correctly but with a weaker intralayer interaction parameter. We attribute this to the higher value of $U=8$ eV needed to obtain the experimental band gap of ilmenite. The magnetic interaction parameters between Fe^{3+} and Fe^{2+} at the interface of hematite-ilmenite, extracted here, are dominated by a strong antiferromagnetic coupling between the interfacial Fe^{2+} and Fe^{3+} from the next hematite layer, similar to the end member hematite. Although the absolute values are lower than in hematite, the negative sign fixes the orientation of defect spins at the interface leading to a ferrimagnetic behavior in the heterostructure.

ACKNOWLEDGMENTS

Funding by the DFG (Grant No. Pe883/4-1), ESF (EuroMinSci), and computational time at the Leibniz Rechenzentrum are gratefully acknowledged.

---

*hasan.sadat@lrz.uni-muenchen.de

[1] Y. Ishikawa and S. Akimoto, J. Phys. Soc. Jpn. **12**, 1083 (1957).

[2] P. Robinson, R. J. Harrison, S. A. McEnroe, and R. B. Hargraves, Nature (London) **418**, 517 (2002).

[3] R. Pentcheva and H. Sadat Nabi, Phys. Rev. B **77**, 172405 (2008).

[4] U. Falk, A. Furrer, H. U. Güdel, and J. K. Kjems, Phys. Rev. B **35**, 4888 (1987).

[5] U. Falk, A. Furrer, N. Furer, H. U. Güdel, and J. K. Kjems, Phys. Rev. B **35**, 4893 (1987).

[6] F. Mila, P. Millet, and J. Bonvoisin, Phys. Rev. B **54**, 11925 (1996).

[7] W. E. Pickett, Phys. Rev. Lett. **79**, 1746 (1997).

[8] M. P. Gelfand, Z. Weihong, R. R. P. Singh, J. Oitmaa, and C. J. Hamer, Phys. Rev. Lett. **77**, 2794 (1996).

[9] S. Shi, A. L. Wysocki, and K. D. Belashchenko, Phys. Rev. B **79**, 104404 (2009).

[10] O. Le Bacq, A. Pasturel, C. Lacroix, and M. D. Núñez-Regueiro, Phys. Rev. B **71**, 014432 (2005).

[11] A. I. Liechtenstein, M. I. Katsnelson, V. P. Antropov, and V. A. Gubanov, J. Magn. Magn. Mater. **67**, 65 (1987).

[12] S. Picozzi and M. Ležaić, New J. Phys. **10**, 055017 (2008).

[13] E. J. Samuelsen and G. Shirane, Phys. Status Solidi **42**, 241 (1970).

[14] E. J. Samuelsen and G. Shirane, J. Phys. Colloq. **32**, 1064 (1971).

[15] H. Kato, S. Funahashi, Y. Yamaguchi, M. Yamada, and H. Takei, J. Magn. Magn. Mater. **31-34**, 617 (1983).

[16] H. Kato, Y. Yamaguchi, M. Yamada, S. Funahashii, Y. Nakagawa, and H. Takei, J. Phys. C **19**, 6993 (1986).

[17] V. V. Mazurenko and V. I. Anisimov, Phys. Rev. B **71**, 184434 (2005).

[18] P. Blaha, K. Schwarz, G. K. H. Madsen, D. Kvasnicka, and J. Luitz, *WIEN2k, An Augmented Plane Wave Plus Local Orbitals Program for Calculating Crystal Properties* (Technische Universität Wien, Austria, 2001).

[19] J. P. Perdew, K. Burke, and M. Ernzerhof, Phys. Rev. Lett. **77**, 3865 (1996).

[20] V. I. Anisimov, I. V. Solovyev, M. A. Korotin, M. T. Czyžyk, and G. A. Sawatzky, Phys. Rev. B **48**, 16929 (1993).

[21] G. Rollmann, A. Rohrbach, P. Entel, and J. Hafner, Phys. Rev. B **69**, 165107 (2004).

[22] I. Leonov, A. N. Yaresko, V. N. Antonov, M. A. Korotin, and V. I. Anisimov, Phys. Rev. Lett. **93**, 146404 (2004).

[23] H.-T. Jeng, G. Y. Guo, and D. J. Huang, Phys. Rev. Lett. **93**, 156403 (2004).

[24] H. P. Pinto and S. D. Elliot, J. Phys.: Condens. Matter **18**, 10427 (2006).

[25] V. I. Anisimov and O. Gunnarsson, Phys. Rev. B **43**, 7570 (1991).

[26] G. K. H. Madsen and P. Novak, Europhys. Lett. **69**, 777 (2005).

[27] D. A. Perkins and J. P. Attfield, J. Chem. Soc., Chem. Commun. **4**, 229 (1991).

[28] R. J. Harrison, S. A. T. Redefern, and R. I. Smith, Am. Mineral. **85**, 194 (2000).

[29] F. Tran, J. Kunes, P. Novak, P. Blaha, and L. D. Marks, Comput. Phys. Commun. **179**, 784 (2008).

[30] J. B. Goodenough, Phys. Rev. **117**, 1442 (1960).

[31] P. W. Anderson, Phys. Rev. **115**, 2 (1959).

[32] L. M. Sandratskii, M. Uhl, and J. Kübler, J. Phys.: Condens. Matter **8**, 983 (1996).

[33] A. H. Morrish, *Canted Antiferromagnetism: Hematite* (World Scientific, Singapore, 1994).

[34] J. Kuneš, Dm. M. Korotin, M. A. Korotin, V. I. Anisimov and P. Werner, Phys. Rev. Lett. **102**, 146402 (2009).

[35] R. J. Harrison, Am. Mineral. **91**, 1006 (2006).

[36] R. J. Harrison, S. A. McEnroe, P. Robinson, B. Carter-Stiglitz, E. J. Palin, and T. Kasama, Phys. Rev. B **76**, 174436 (2007).

[37] H. Sadat Nabi and R. Pentcheva, J. Appl. Phys. **106**, 073912 (2009).